

Design of low-alloying and high-performance solid solution-strengthened copper alloys with element substitution for sustainable development

Jiaqiang Li, Hongtao Zhang, Jingtai Sun, Huadong Fu, and Jianxin Xie

Cite this article as:

Jiaqiang Li, Hongtao Zhang, Jingtai Sun, Huadong Fu, and Jianxin Xie, Design of low-alloying and high-performance solid solution-strengthened copper alloys with element substitution for sustainable development, *Int. J. Miner. Metall. Mater.*, 31(2024), No. 5, pp. 826-832. <https://doi.org/10.1007/s12613-024-2870-3>

View the article online at [SpringerLink](#) or [IJMMM Webpage](#).

Articles you may be interested in

Xiao-chun Wen, Lei Guo, Qi-peng Bao, and Zhan-cheng Guo, [Rapid removal of copper impurity from bismuth–copper alloy melts via super-gravity separation](#), *Int. J. Miner. Metall. Mater.*, 28(2021), No. 12, pp. 1929-1939. <https://doi.org/10.1007/s12613-020-2118-9>



IJMMM WeChat



QQ author group

Design of low-alloying and high-performance solid solution-strengthened copper alloys with element substitution for sustainable development

Jiaqiang Li¹⁾, Hongtao Zhang^{1,2,3),✉}, Jingtai Sun^{1,2,3)}, Huadong Fu^{1,2,3,4)}, and Jianxin Xie^{1,2,3),✉}

1) Beijing Advanced Innovation Center for Materials Genome Engineering, University of Science and Technology Beijing, Beijing 100083, China

2) Key Laboratory for Advanced Materials Processing (MOE), University of Science and Technology Beijing, Beijing 100083, China

3) Beijing Laboratory of Metallic Materials and Processing for Modern Transportation, University of Science and Technology Beijing, Beijing 100083, China

4) Liaoning Academy of Materials, Shenyang 110004, China

(Received: 10 October 2023; revised: 21 January 2024; accepted: 27 February 2024)

Abstract: Solid solution-strengthened copper alloys have the advantages of a simple composition and manufacturing process, high mechanical and electrical comprehensive performances, and low cost; thus, they are widely used in high-speed rail contact wires, electronic component connectors, and other devices. Overcoming the contradiction between low alloying and high performance is an important challenge in the development of solid solution-strengthened copper alloys. Taking the typical solid solution-strengthened alloy Cu–4Zn–1Sn as the research object, we proposed using the element In to replace Zn and Sn to achieve low alloying in this work. Two new alloys, Cu–1.5Zn–1Sn–0.4In and Cu–1.5Zn–0.9Sn–0.6In, were designed and prepared. The total weight percentage content of alloying elements decreased by 43% and 41%, respectively, while the product of ultimate tensile strength (UTS) and electrical conductivity (EC) of the annealed state increased by 14% and 15%. After cold rolling with a 90% reduction, the UTS of the two new alloys reached 576 and 627 MPa, respectively, the EC was 44.9%IACS and 42.0%IACS, and the product of UTS and EC (UTS × EC) was 97% and 99% higher than that of the annealed state alloy. The dislocations proliferated greatly in cold-rolled alloys, and the strengthening effects of dislocations reached 332 and 356 MPa, respectively, which is the main reason for the considerable improvement in mechanical properties.

Keywords: element substitution; copper alloy; solid solution strengthening; microstructure and performance

1. Introduction

Copper alloys have excellent mechanical and electrical properties, finding extensive applications in electronic components, railway transit, automobile manufacturing, aerospace, and various other industries [1–2]. Among these alloys, solid solution-strengthened copper alloys have the advantages of a simple composition and manufacturing process, low cost, and so on, and are widely applied in high-speed rail contact wires, electronic component connectors, and other fields [3–4]. For example, Cu–0.4Mg alloy is widely used in high-speed rail contact wires, and Cu–Zn–Sn alloy, represented by Cu–4Zn–1Sn, is widely used in instrument clips, fuse clips, relay springs, and other devices [4]. Alloying is one of the most important means to improve the strength of solid solution-strengthened copper alloys and regulate their comprehensive properties [5–6]. For example, increasing the content of solid solution elements such as Ni [7], Fe [8], Sn [9], and Zn [10] in copper alloys can substantially improve alloy strength. However, the increase in alloying degree will complicate the alloy manufacturing process and increase the environmental burden and difficulty of recycling, which is not conducive to the sustainable development of metal materials. Therefore, breaking through the contradiction between high

performance and low alloying of metal materials has recently become a focus of widespread concern and a major research topic [11–12]. For example, Li and Lu [13–14] and Raabe *et al.* [12] proposed improving alloy performance and reducing alloying by regulating the microstructure and defects of an alloy. They adopted nano-twin to considerably improve the mechanical properties of copper. We believe that if we can screen out the alloying element with a greater effect of solid solution strengthening and a smaller effect on electrical conductivity (EC), we can design new copper alloys or partially/completely replace the alloying elements in existing solid solution-strengthened copper alloys, which may also effectively reduce the total content of elements in alloys and break through the contradiction between low alloying and high performance.

In our previous work [15], we found that among all the solid solution strengthening elements of copper alloys with a solid solubility of >0.1wt% at room temperature, In is the alloying element with the best solid solution strengthening effect and the least influence on the EC reduction. Various Cu–In solid solution-strengthened copper alloys with excellent comprehensive properties were designed. In this paper, we proposed a new low-alloying design idea using In to partially replace the alloying elements in a conventional solid

✉ Corresponding authors: Hongtao Zhang E-mail: zht@ustb.edu.cn; Jianxin Xie E-mail: jxxie@mater.ustb.edu.cn

© University of Science and Technology Beijing 2024

solution-strengthened copper alloy, substantially reducing the total amount of alloying elements while ensuring or even improving the overall performance. Taking the typical solid solution-strengthened Cu–4Zn–1Sn alloy as the object, we explored the possibility of adding a small amount of In to greatly reduce the content of Zn and analyzed the microstructure and performance of the new alloy after elemental substitution. The work of this paper provides a new way to reduce the total content of elements in metal alloys and promote the sustainable development of metal materials.

2. Experimental

With Cu–4Zn–1Sn (OS025, ultimate tensile strength (UTS) of 280 MPa, EC of 41%IACS) [4] alloy as the benchmark alloy, the total content of alloying elements was greatly reduced in this research by adding a small amount of In. Initially, using the machine learning model constructed in our previous work [15], the effects of different Zn, Sn, and In

contents on the mechanical and electrical properties of the alloy were predicted. Two Cu–Zn–Sn–In alloys with properties not lower than the benchmark alloy and a substantial reduction in the total content of alloying elements were designed. The compositions are shown in Table 1.

Alloy ingots of 150 mm × 80 mm × 80 mm in size were prepared using vacuum medium frequency induction melting. After removing the surface oxide layer and defects of ingots, homogenization heat treatment at 600°C for 24 h was performed in a KSL-1200X box furnace. After removing the surface oxide layer, samples were cold rolled at 90% deformation. The cold-rolled samples were recrystallized at 600°C for 20 min in the KSL-1200X box furnace. The grain size was controlled to be approximately 25 μm, basically consistent with the OS025 state in Reference [4]. The recrystallization annealing samples were cold rolled with deformation of 50%, 70%, and 90%. The performance test and microstructure observation of annealed and cold-rolled alloys were performed.

Table 1. Chemical composition of Cu–Sn–Zn–In alloy

Alloy	Design composition			Measured composition				wt%
	Zn	Sn	In	Cu	Zn	Sn	In	
Cu–1.5Zn–1Sn–0.4In	1.5	1	0.4	Bal.	1.48	1	0.35	Bal.
Cu–1.5Zn–0.9Sn–0.6In	1.5	0.9	0.6	Bal.	1.44	0.9	0.62	Bal.

According to GB/T228.1-2010, the dog-bone-shaped samples and a gauge length of 20 mm were prepared. The mechanical properties of the tensile samples at room temperature were tested using an MTS universal material testing machine. The displacement rate of the tensile chuck was 1 mm/min. The EC of the alloy samples was measured using a Sigma2008B digital eddy current metal conductivity meter. Each sample was measured six times, and the average value was taken as the experimental value of the EC. The metallographic structure of the sample was observed using a ZEISS Axio Imager.A2m metallographic microscope, and the grain size was counted by Image-pro. The metallographic structure observation sample corrosion solution ratio of hydrochloric acid ferric chloride solution is $\text{FeCl}_3 : \text{HCl} : \text{H}_2\text{O} = 5 \text{ g} : 10 \text{ mL} : 90 \text{ mL}$. The phase composition and microstrain of the alloy were analyzed using a D5000 X-ray diffractometer. The grain boundary, orientation, and strain of the alloy were observed using electron backscatter diffraction (EBSD) of a JSM-7900F field scanning electron microscope.

3. Results and analysis

3.1. Properties of Cu–Sn–Zn–In alloy

Fig. 1 shows the stress–strain curves of the two types of Cu–Sn–Zn–In alloys designed in this paper after recrystallization annealing heat treatment. This figure shows that the UTS of Cu–1.5Zn–1Sn–0.4In is (283 ± 3) MPa, the yield strength (YS) is (88 ± 1) MPa, the break elongation (EL) is $(57.7 \pm 2.8)\%$, and the EC is $(46.3 \pm 0.7)\%$ IACS; the UTS, YS, EL, and EC of Cu–1.5Zn–0.9Sn–0.6In are (299 ± 1)

MPa, (101 ± 4) MPa, $(57.5 \pm 4.0)\%$, and $(44.2 \pm 0.8)\%$ IACS, respectively. Compared with the benchmark alloy Cu–4Zn–1Sn, the two new alloys have similar mechanical properties and a considerably improved EC. The Cu–1.5Zn–1Sn–0.4In and Cu–1.5Zn–0.9Sn–0.6In alloys showed a substantial increase in the UTS × EC, by 14% and 15%, respectively, while the total alloying element content was greatly reduced, by 43% and 41%, respectively.

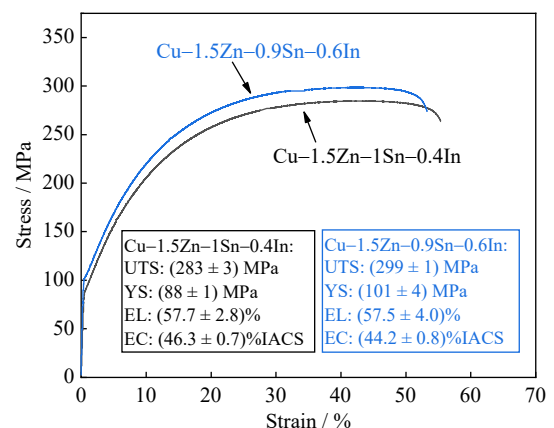


Fig. 1. Mechanical properties of the annealed Cu–Sn–Zn–In alloys (Comparison: OS025 temper Cu–4Zn–1Sn, UTS = 280 MPa, EC = 41%IACS [4]).

Then, the annealed state Cu–Sn–Zn–In alloys were cold rolled with different deformations, and the strength and EC of the samples were tested. The results are shown in Fig. 2. This figure shows that the UTS and YS of the two new alloys after cold rolling are considerably improved, the EL after fracture

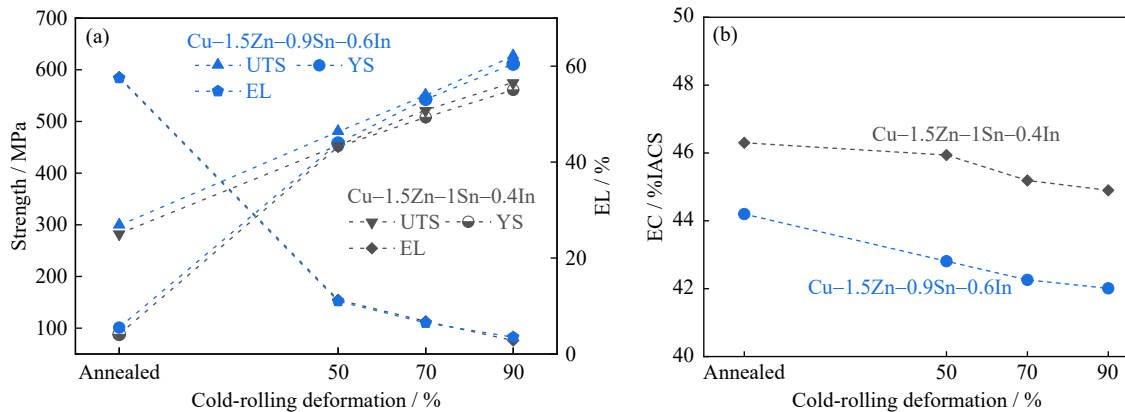


Fig. 2. Change in the properties of two Cu-Sn-Zn-In alloys with cold-rolling deformation: (a) mechanical properties; (b) electrical conductivity.

is substantially reduced, and the EC is slightly reduced. Fig. 2(a) shows that the UTS and YS of the Cu-1.5Zn-1Sn-0.4In alloy sample increase rapidly from (283 ± 3) MPa and (88 ± 1) MPa in the annealed state to (576 ± 5) MPa and (561 ± 2) MPa after the 90% cold-rolling deformation, respectively. The UTS and YS of the Cu-1.5Zn-0.9Sn-0.6In alloy sample increase rapidly from (299 ± 1) MPa and (101 ± 4) MPa in the annealed state to (627 ± 4) MPa and (611 ± 3) MPa after the 90% cold-rolling deformation. These results show that the cold-rolling deformation strengthening effect of the two new alloys is very considerable, and the mechanical properties of the alloys can be controlled in a large range by cold deformation to meet the needs of different application scenarios. The ELs after fracture of the two new alloy samples decrease rapidly from more than 57% in the annealed state to approximately 11% after the 50% cold-rolling deformation and approximately 3% after the 90% cold-rolling deformation.

Fig. 2(b) shows that with increasing deformation, cold working has little effect on the ECs of the two new alloy samples. The EC of the Cu-1.5Zn-1Sn-0.4In alloy sample decreases from $(46.3 \pm 0.7)\%$ IACS in the annealed state to $(44.9 \pm 0.2)\%$ IACS after 90% cold-rolling deformation, a decrease of only 1.4 percentage points. The EC of the Cu-1.5Zn-0.9Sn-0.6In alloy sample decreases from $(44.2 \pm 0.8)\%$ IACS in the annealed state to $(42.0 \pm 0.3)\%$ IACS after the 90% cold-rolling deformation, a decrease of only 2.2 percentage points.

According to comprehensive consideration of the strength and EC of the solid solution-strengthened copper alloys, cold rolling substantially improves the overall performance of the new alloy sample. Compared to the annealed state, Cu-1.5Zn-1Sn-0.4In alloy and Cu-1.5Zn-0.9Sn-0.6In alloy after cold rolling with 90% reduction increased by 97% and 99% in the UTS \times EC, respectively.

3.2. Microstructure of Cu-Sn-Zn-In alloy

The metallographic microstructures of the two Cu-Sn-Zn-In alloys after the recrystallization annealing treatment are shown in Fig. 3. This diagram shows that the recrystallized grains of the two new alloys are equiaxed, and more annealing twins appear in the grains. The average grain sizes of

Cu-1.5Zn-1Sn-0.4In and Cu-1.5Zn-0.9Sn-0.6In alloys are $24.7 \mu\text{m}$ and $26.6 \mu\text{m}$, respectively, very near $25 \mu\text{m}$ for the benchmark alloy Cu-4Zn-1Sn [4].

Fig. 4 shows the EBSD structure of a Cu-Sn-Zn-In alloy sample after 90% cold-rolling deformation with a step size of

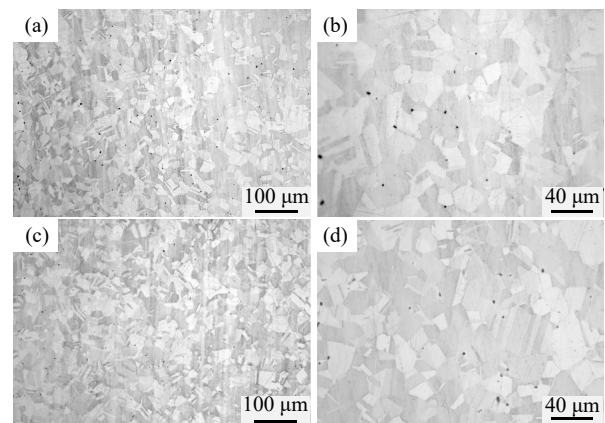


Fig. 3. Metallographic graphs of the two new alloys after recrystallization annealing: (a, b) Cu-1.5Zn-1Sn-0.4In alloy; (c, d) Cu-1.5Zn-0.9Sn-0.6In alloy.

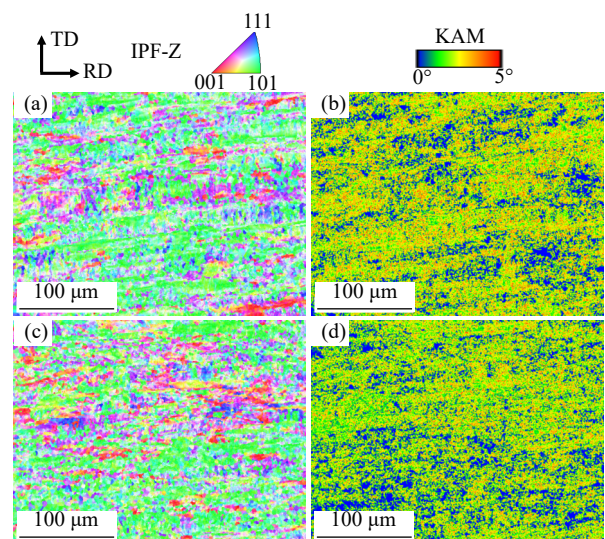


Fig. 4. EBSD microstructure of the two new alloy samples after 90% cold rolling: (a, b) Cu-1.5Zn-1Sn-0.4In alloy; (c, d) Cu-1.5Zn-0.9Sn-0.6In alloy. TD—transverse direction; RD—rolling direction.

0.5 μm and resolutions of 93% and 89%. The inverse pole figure (IPF) results of Fig. 4(a) and (c) show that after cold rolling, the grains of the two new alloy samples are flattened and below 10 μm in width. The kernel average misorientation (KAM) results of Fig. 4(b) and (d) show that the grains in the alloy sample have a large strain after cold rolling. After 90% cold rolling, the two new alloy samples have basically identical grain sizes and strain degrees.

The grain size of the cold-rolled alloy sample with 90%

deformation was further analyzed, and the results are shown in Fig. 5. The resolutions of Fig. 5(a), (b, c), (d), and (e, f) are 93%, 96%, 89%, and 95%, respectively, and the large-angle grain boundaries are set to ≥15°. This figure shows that after cold rolling, the two new alloys have flat grains and identical grain size distribution characteristics. The size is between 2 and 40 μm and usually less than 5 μm. The average grain size is 3.6 μm for the Cu–1.5Zn–1Sn–0.4In alloy and 3.4 μm for the Cu–1.5Zn–0.9Sn–0.6In alloy.

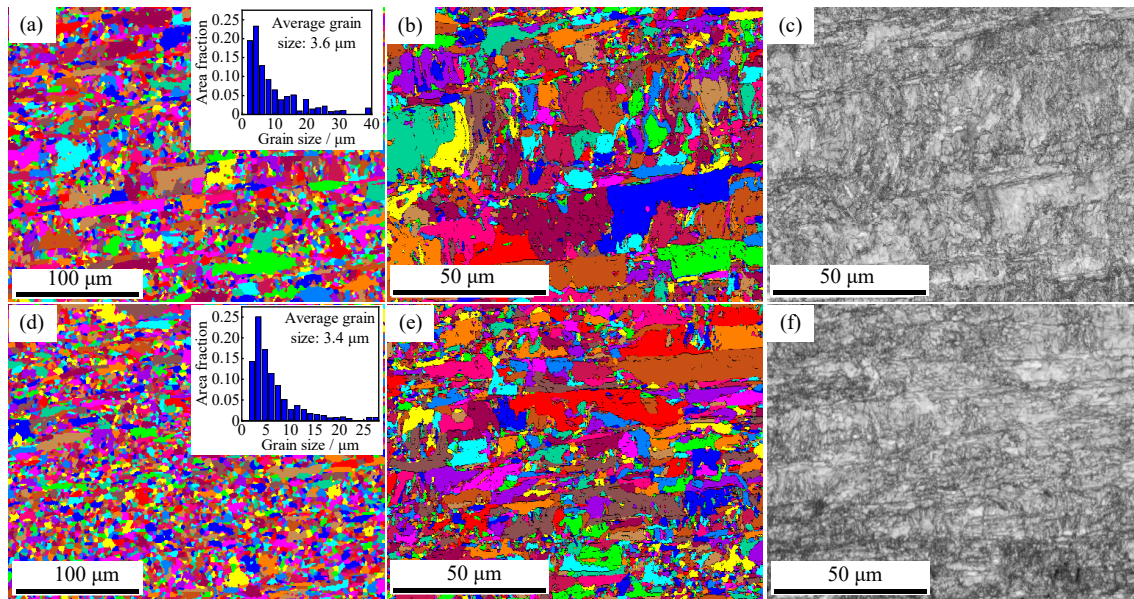


Fig. 5. Grain size distribution of the Cu–Sn–Zn–In alloy after 90% cold rolling: (a) grain map of Cu–1.5Zn–1Sn–0.4In alloy with a step size of 0.5 μm; (b) grain map and (c) image quality map of Cu–1.5Zn–1Sn–0.4In alloy with a step size of 0.15 μm; (d) grain map of Cu–1.5Zn–0.9Sn–0.6In alloy with a step size of 0.5 μm; (e) grain map and (f) image quality map of Cu–1.5Zn–0.9Sn–0.6In alloy with a step size of 0.15 μm. Inset in (a) and (d) are grain size distribution results.

4. Discussion

4.1. Effect of In element replacing Zn and Sn elements

The two new low-alloying alloys Cu–1.5Zn–1Sn–0.4In and Cu–1.5Zn–0.9Sn–0.6In designed in this study have a UTS and EC in the annealed state of 283 MPa and 46.3%IACS and 299 MPa and 44.2%IACS, respectively. Compared with the benchmark alloy Cu–4Zn–1Sn (UTS = 280 MPa and EC = 41%IACS [4]), the Cu–1.5Zn–1Sn–0.4In alloy is almost identical in UTS and higher in EC by 5.3 percentage points. The UTS of Cu–1.5Zn–0.9Sn–0.6In alloy is increased by 19 MPa, and the EC is increased by 3.2 percentage points. These results show that compared with the benchmark, the total content of alloying elements in the two new alloys Cu–1.5Zn–1Sn–0.4In and Cu–1.5Zn–0.9Sn–0.6In is reduced by 43% and 41%, respectively, while the UTS × EC is increased by 14% and 15%, respectively. The low-alloying effect of using In instead of Zn and Sn is very important.

Fig. 6 compares the properties of the new low-alloying alloy designed in this paper with other OS025 temper solid solution-strengthened copper alloys in the copper alloy manual [4]. The blue dots in the figure are the UTS and EC of existing solid-solution strengthened alloys such as Cu–Zn,

Cu–Sn, and Cu–Ni, and the blue dotted line represents the boundary between the comprehensive properties of the alloy. Substantially improving the overall performance while greatly reducing the total content of alloying elements is an important challenge for the sustainable development of solid solution-strengthened copper alloys. This work provides a new idea for addressing this challenge.

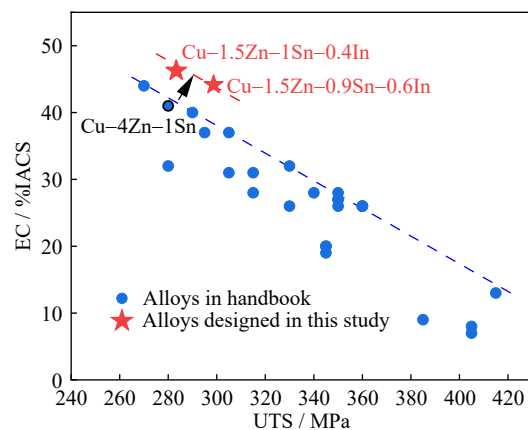


Fig. 6. Performance comparison between the new low-alloying alloy designed in this paper and the solid solution-strengthened copper alloys in the handbook [4].

4.2. Strengthening effect of Cu–Sn–Zn–In alloy

The new low-alloying copper alloy designed in this paper has excellent mechanical properties after cold rolling with 90% deformation. Its main strengthening methods include solid solution strengthening, grain boundary strengthening, and dislocation strengthening, as shown in Eq. (1).

$$\sigma_y = \sigma_0 + \sigma_s + \sigma_d + \sigma_g \quad (1)$$

where σ_0 is the lattice friction stress, which is 25 MPa for copper [16–17]. σ_s , σ_d , and σ_g are solid solution strengthening, dislocation strengthening, and grain boundary strengthening, respectively.

According to the classical solid solution strengthening theory of a Labusch homogeneous solid solution, the relationship between the YS (σ_{ys}) of a solid solution and the concentration of solute atoms is shown in Eq. (2) [18–19].

$$\sigma_{ys} = \sigma_{y0} + Z_L G (\alpha^2 \delta^2 + \eta^2)^{2/3} c^{2/3} \quad (2)$$

where σ_{y0} is the yield strength of pure metal, c is the solute concentration, Z_L and α are constants, and G is the shear modulus of a solid solution, which is 45.5 GPa [20]. δ is the size mismatch, as shown in Eq. (2), and η is the modulus mismatch, as shown in Eq. (3) [21].

$$\delta = a^{-1} \frac{da}{dc} \quad (3)$$

where a is the lattice constant, which is 0.361 nm for copper.

$$\eta = 2(G_1 - G_0)/(G_1 + G_0) \quad (4)$$

where G_0 is the shear modulus of the solvent atom, and G_1 is the shear modulus of the solute atom.

For the two Cu–Zn–Sn–In alloys designed in this paper, the atomic concentrations of Sn, Zn, and In are 0.54at%,

1.45at%, and 0.19at%, and 0.49at%, 1.41at%, and 0.35at%, respectively. According to the above theoretical formulas, the solid solution strengthening effects of Sn and Zn (σ_{s-Sn} and σ_{s-Zn}) in Cu–1.5Zn–1Sn–0.4In and Cu–1.5Zn–0.9Sn–0.6In alloys are calculated as 41 and 25 MPa and 38 and 25 MPa, respectively. Because the shear modulus of In is unknown, the above theoretical calculation cannot be performed directly. Then, the solid solution strength of In is obtained from the difference between the YS of the two alloys. The solid solution strengthening effects of In (σ_{s-In}) is approximately 20 MPa for Cu–1.5Zn–1Sn–0.4In and approximately 30 MPa for Cu–1.5Zn–0.9Sn–0.6In.

Dislocation strengthening can be calculated using Eq. (5) [22] as follows.

$$\sigma_d = M G a b \sqrt{\rho} \quad (5)$$

where α is 0.2 for copper alloy. ρ is the dislocation density, calculated according to the formula $\frac{16.1 \times \varepsilon^2}{b^2}$. Here, ε is the microstrain, obtained from XRD results, and b is the Burgers vector, which is 0.255 nm.

Fig. 7 shows the XRD results of the two new alloys designed after cold rolling with 90% deformation. The marked diffraction peaks all belong to Cu, indicating that the Cu–Sn–Zn–In alloy is a solid solution with Cu as the matrix, and the second phases are not numerous. In contrast, the microstrains of Cu–1.5Zn–1Sn–0.4In and Cu–1.5Zn–0.9Sn–0.6In alloys were calculated to be 0.297 and 0.319, respectively, and the dislocation densities were calculated to be 2.18×10^{15} and 2.52×10^{15} , respectively. According to Eq. (5), the dislocation strengthening effects were calculated to be 332 and 356 MPa, respectively.

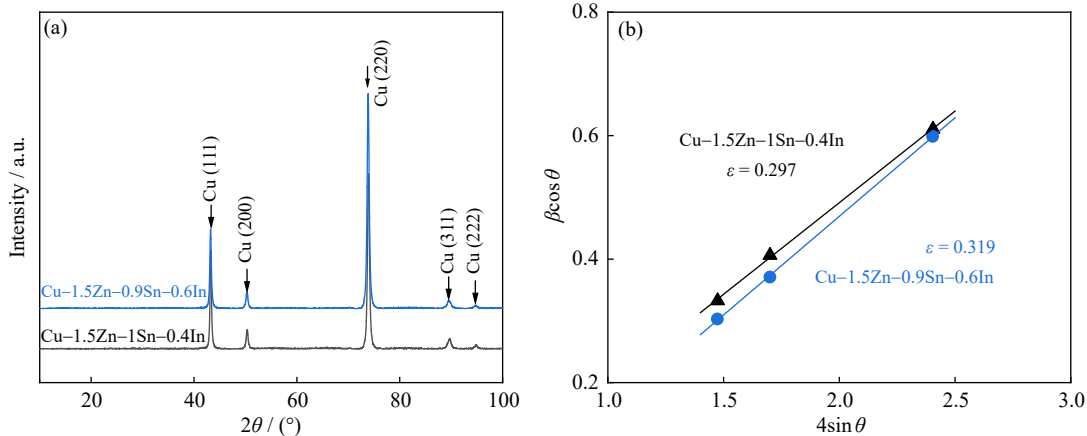


Fig. 7. (a) XRD results and (b) microstrain (ε) fitting of cold-rolled Cu–Sn–Zn–In alloy with 90% deformation. β is the width at half height of the XRD diffraction peak.

Grain boundary strengthening can be calculated according to the Hall–Petch [23–24] relationship, as shown in Eq. (6):

$$\sigma_g = K d^{-1/2} \quad (6)$$

where d is the average grain size, and K is a constant, being 0.18 MPa·m^{1/2} [25]. According to the grain size shown in Fig. 5, the grain boundary strengthening effects of Cu–

1.5Zn–1Sn–0.4In and Cu–1.5Zn–0.9Sn–0.6In alloys are calculated to be 95 and 98 MPa, respectively.

Table 2 shows the experimental results of the strengthening effect and YS of the alloy obtained according to the above theoretical calculation. It shows that the solid solution strengthening effect is only 25 MPa for 1.5wt% alloying element Zn in Cu–Zn–Sn–In alloy but reaches 20 and 30 MPa for 0.4wt% and 0.6wt% alloying element In in the alloy, re-

spectively. In terms of the solid solution strengthening effects of Sn, Zn, and In, Zn is the lowest and In is the highest. This result is consistent with the order of the solid solution strengthening effect of elements determined by the author's previous research group (Fig. 3(e) of Reference [15]) and the

theoretical calculation results in relevant literature [26–27]. The above results prove the feasibility of replacing a small amount of Sn and more Zn with a small amount of In, and the new alloy still maintains high mechanical properties after the replacement design.

Table 2. Calculation results of the strengthening effect of Cu–Sn–Zn–In alloy

MPa

Alloy	σ_0	σ_{s-Sn}	σ_{s-Zn}	σ_{s-In}	σ_d	σ_g	σ_{y-cal}	σ_{y-test}
Cu–1.5Zn–1Sn–0.4In	25	41	25	20	332	95	538	561
Cu–1.5Zn–0.9Sn–0.6In	25	38	25	30	356	98	572	611

Note: σ_{y-cal} and σ_{y-test} represent the calculated YS and measured YS, respectively.

In addition, after cold rolling with 90% deformation, many dislocations proliferate in the alloy samples, and the strengthening effects in the two new alloys Cu–1.5Zn–1Sn–0.4In and Cu–1.5Zn–0.9Sn–0.6In reach 332 and 356 MPa, respectively, accounting for 59% and 58% of the YS of the alloy, respectively, the main reason for the substantial improvement in the mechanical properties of the alloy.

5. Conclusions

In this paper, the alloy element In with a high solid solution strengthening effect and low conductivity reduction was proposed to partially replace Zn and Sn in the typical solid solution-strengthened copper alloy Cu–4Zn–1Sn, realizing the design of low-alloying and high-performance copper alloys. The microstructure and mechanical–electrical properties of the two newly designed alloys were studied. The main results are as follows.

(1) Two new alloys, Cu–1.5Zn–1Sn–0.4In and Cu–1.5Zn–0.9Sn–0.6In, were designed and prepared. Compared with the benchmark alloy Cu–4Zn–1Sn, the content of alloying elements in the new alloys decreased by 43% and 41%, respectively, and the UTS \times EC of annealed specimens increased by 14% and 15%, respectively.

(2) After cold rolling with 90% deformation, UTS reached 576 and 627 MPa for Cu–1.5Zn–1Sn–0.4In and Cu–1.5Zn–0.9Sn–0.6In alloys, respectively, and the EC values were 44.9%IACS and 42.0%IACS, respectively; the UTS \times EC increased by 97% and 99%, respectively, compared with the annealed specimens; the dislocations proliferated greatly in cold-rolled samples, and their strengthening effects reached 332 and 356 MPa, respectively.

(3) Among the three elements Sn, Zn, and In, the solid solution strengthening effect of Zn is the lowest and In is the highest. Therefore, the new alloys still maintain a high combination property by replacing a small amount of Sn with more Zn and using a small amount of In.

Acknowledgements

This work was financially supported by the National Key Research and Development Program of China (No. 2021YFB3803101), the National Natural Science Foundation of China (Nos. 52022011, 51974028, and 52090041),

the Xiaomi Young Scholars Program, and China National Postdoctoral Program for Innovative Talents (No. BX 20230042).

Conflict of Interest

Jianxin Xie is an advisory member for this journal and was not involved in the editorial review or the decision to publish this article. All authors state that there is no conflict of interest. The authors declare no conflict of interest.

References

- [1] Y.X. Jiang, H.F. Lou, H.F. Xie, *et al.*, Development status and prospects of advanced copper alloy, *Strategic Study of CAE*, 22(2020), No. 5, p. 84.
- [2] C.Z. Huang, Y.B. Jiang, Z.X. Wu, *et al.*, Significantly enhanced high-temperature mechanical properties of Cu–Cr–Zn–Zr–Si alloy with stable second phases and grain boundaries, *Mater. Des.*, 233(2023), art. No. 112292.
- [3] K. Maki, Y. Ito, H. Matsunaga, and H. Mori, Solid-solution copper alloys with high strength and high electrical conductivity, *Scripta Mater.*, 68(2013), No. 10, p. 777.
- [4] J.R. Davis, *ASM Specialty Handbook: Copper and Copper Alloys*, ASM International, Ohio, 2001.
- [5] H. Zhang, X.C. Deng, and G.H. Zhang, Preparation and properties of multiphase solid-solution strengthened high-performance W–Cu alloys through alloying with Mo, Fe and Ni, *Mater. Sci. Eng. A*, 871(2023), art. No. 144909.
- [6] S.W. Huang, P.F. Zhou, F.X. Luo, *et al.*, Effects of Ni and Mn contents on precipitation and strengthening behavior in Cu–Ni–Mn ternary alloys, *Mater. Charact.*, 199(2023), art. No. 112775.
- [7] J.Y. Wang, X.Q. Lü, S.Q. Chen, Y. Gao, and Y. Liu, Effect of Ni content on the solid solution strengthening behavior of Cu–Ni–Ag alloys, *Mater. Sci. Eng. Powder Metall.*, 26(2021), No. 3, p. 263.
- [8] R.W. Liao, L.R. Wang, X.Z. Liu, and Y. Liu, Microstructure and properties of Cu–Zn–Al–Fe alloy, *Hot Working Technol.*, 48(2019), No. 16, p. 75.
- [9] P. Yang, D.Y. He, W. Shao, *et al.*, Study of the microstructure and mechanical properties of Cu–Sn alloys formed by selective laser melting with different Sn contents, *J. Mater. Res. Technol.*, 24(2023), p. 5476.
- [10] E. Bruder, P. Braun, H.U. Rehman, *et al.*, Influence of solute effects on the saturation grain size and rate sensitivity in Cu–X alloys, *Scripta Mater.*, 144(2018), p. 5.
- [11] E.A. Olivetti and J.M. Cullen, Toward a sustainable materials system, *Science*, 360(2018), No. 6396, p. 1396.
- [12] D. Raabe, C.C. Tasan, and E.A. Olivetti, Strategies for improv-

- ing the sustainability of structural metals, *Nature*, 575(2019), p. 64.
- [13] X.Y. Li and K. Lu, Playing with defects in metals, *Nat. Mater.*, 16(2017), No. 7, p. 700.
- [14] X.Y. Li and K. Lu, Improving sustainability with simpler alloys, *Science*, 364(2019), No. 6442, p. 733.
- [15] H.T. Zhang, H.D. Fu, X.Q. He, *et al.*, Dramatically enhanced combination of ultimate tensile strength and electric conductivity of alloys via machine learning screening, *Acta Mater.*, 200(2020), p. 803.
- [16] S.S. Zhang, H.H. Zhu, L. Zhang, W.Q. Zhang, H.Q. Yang, and X.Y. Zeng, Microstructure and properties in QCr0.8 alloy produced by selective laser melting with different heat treatment, *J. Alloys Compd.*, 800(2019), p. 286.
- [17] X.W. Zuo, K. Han, C.C. Zhao, R.M. Niu, and E.G. Wang, Microstructure and properties of nanostructured Cu28wt%Ag microcomposite deformed after solidifying under a high magnetic field, *Mater. Sci. Eng. A*, 619(2014), p. 319.
- [18] T.P. Harzer, S. Djaziri, R. Raghavan, and G. Dehm, Nanostructure and mechanical behavior of metastable Cu–Cr thin films grown by molecular beam epitaxy, *Acta Mater.*, 83(2015), p. 318.
- [19] A. Akhtar and E. Teghtsoonian, Substitutional solution hardening of magnesium single crystals, *Philos. Mag.*, 25(1972), No. 4, p. 897.
- [20] J.Z. Li, H. Ding, B.M. Li, W.L. Gao, J. Bai, and G. Sha, Effect of Cr and Sn additions on microstructure, mechanical-electrical properties and softening resistance of Cu–Cr–Sn alloy, *Mater. Sci. Eng. A*, 802(2021), art. No. 140628.
- [21] H.E. Friedrich and B.L. Mordike, *Magnesium technology*, Springer-Verlag Berlin Heidelberg, Berlin, 2006.
- [22] L. Balogh, T. Ungár, Y.H. Zhao, *et al.*, Influence of stacking-fault energy on microstructural characteristics of ultrafine-grain copper and copper–zinc alloys, *Acta Mater.*, 56(2008), No. 4, p. 809.
- [23] Y. Zhang, N.R. Tao, and K. Lu, Mechanical properties and rolling behaviors of nano-grained copper with embedded nanotwin bundles, *Acta Mater.*, 56(2008), No. 11, p. 2429.
- [24] N. Hansen, Hall–Petch relation and boundary strengthening, *Scripta Mater.*, 51(2004), No. 8, p. 801.
- [25] Y. Liu, Z. Li, Y.X. Jiang, Y. Zhang, Z.Y. Zhou, and Q. Lei, The microstructure evolution and properties of a Cu–Cr–Ag alloy during thermal-mechanical treatment, *J. Mater. Res.*, 32(2017), No. 7, p. 1324.
- [26] K. Yamaguchi, T. Ishigaki, Y. Inoue, *et al.*, Comprehensive elemental screening of solid-solution copper alloys, *Sci. Technol. Adv. Mater.: Methods*, 3(2023), No. 1, art. No. 2250704.
- [27] Y. Abe, S. Semboshi, N. Masahashi, S.H. Lim, E.A. Choi, and S.Z. Han, Mechanical strength and electrical conductivity of Cu–In solid solution alloy wires, *Metall. Mater. Trans. A*, 54(2023), No. 3, p. 928.